345 Papilledema, IIH and Optic Nerve
Tuesday, May 09, 2017 11:00 AM–12:45 PM
Exhibit/Poster Hall Poster Session
Program #/Board # Range: 3304–3329/B0580–B0605
Organizing Section: Eye Movements/Strabismus/Amblyopia/ Neuro-Ophthalmology

Program Number: 3304 **Poster Board Number:** B0580
Presentation Time: 11:00 AM–12:45 PM
Ultrasonography, OCT and OCT-angiography in the diagnostic workup of children with suspected papilledema
Annegret H. Dahlmann-Noor[1], Gillian G. Adams[3], Moritz C. Daniel[1], Alison Davis[3], Joanne Hancox[3], Melanie Hingorani[3], Patricia Ibanez[4], Becky MacPhee[4], Himanshu Patel[3], Marie Restori[5], Clare Roberts[3], John Sloper[3], Maria Theodorou[3], James Acheson[2].
[1]Paediatric Ophthalmology and Strabismus, NIHR Biomedical Research Centre at Moorfields Eye Hospital and UCL Institute of Ophthalmology, London, United Kingdom; [2]Neuro-ophthalmology, Moorfields Eye Hospital, London, United Kingdom; [3]Paediatric Ophthalmology and Strabismus, Moorfields Eye Hospital, London, United Kingdom; [4]Medical Illustration, Moorfields Eye Hospital, London, United Kingdom; [5]Ocular ultrasound, Moorfields Eye Hospital, London, United Kingdom.
Purpose: Optic nerve sheath dilatation (ONSD) on ocular ultrasound (US) is considered a sensitive and specific indicator of raised intracranial pressure (ICP). Anterior bowing of Bruch membrane (AB-BM) and increase in retinal nerve fibre layer thickness (RNFLT) in superonasal, nasal or temporal sector (SN, N, T) on optical coherence tomography (OCT) may be of similar diagnostic value. OCT-angiography (OCT-A) has not been evaluated in this context. This retrospective observational study explores diagnostic accuracy of US, OCT and OCT-A in children referred for suspected optic nerve head swelling.
Methods: 61 cases assessed over a seven-month period in 2016 at a single centre in London, UK; 26 girls (43%); median age 10.9 years (interquartile range 7.9 to 13). A masked observer collated imaging and clinical data. We calculated specificity and sensitivity for each test; for RNFLT we used published cutoffs as indicators for true optic disc edema: SN: 124, N: 78/74.5, T: 101.5um.
Results: Of 61 cases, three had intracranial pathology: intraventricular tumour (IVT), hypophosphataemic rickets with neuro-imaging signs of chronic raised ICP, and relapse of acute lymphoblastic leukaemia (ALL). All three had symptoms or significant history.
At initial presentation, only one of these three cases had ONSD on ultrasound (sensitivity 33%, specificity 100%). AB-BM had similar accuracy (sensitivity 33%, specificity 96.6%). Increased RNFLT (Fig 1) had higher sensitivity (66.7%), but lower specificity (42.1 to 86%). In all three cases, OCT-A delivered unclear images and could not perform automated measurements of peripapillary vessel density.
Conclusions: In children, ocular ultrasound and OCT alone are not sufficiently accurate to discard the possibility of intracranial pathology. Previous studies have reported that 36.4 to 48% of children with brain tumors or idiopathic intracranial hypertension may not develop papilledema. History and basic neurological assessment remain critical in the diagnostic workup of children with suspected intracranial pathology.

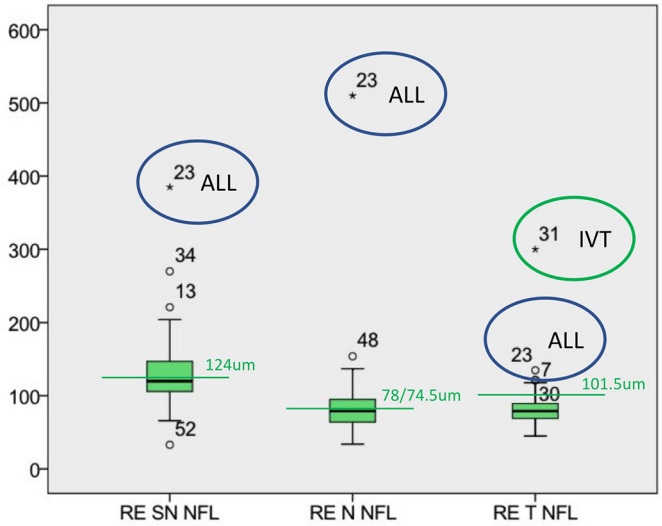

Fig 1. RNFLT (um) superonasal, nasal and temporal sector (right eyes). Case 23 (ALL) had markedly increased RNFLT in the superonasal and nasal sectors. Case 31 (IVT) had marked increase in RFNLT in the temporal sector only. Case 29 (rickets) had no RNFLT increase. Green lines: previously published thresholds for "true papilledema".
Commercial Relationships: Annegret H. Dahlmann-Noor, None; **Gillian G. Adams**, None; **Moritz C. Daniel**, None; **Alison Davis**, None; **Joanne Hancox**, None; **Melanie Hingorani**, None; **Patricia Ibanez**, None; **Becky MacPhee**, None; **Himanshu Patel**, None; **Marie Restori**, None; **Clare Roberts**, None; **John Sloper**, None; **Maria Theodorou**, None; **James Acheson**, None

Program Number: 3305 **Poster Board Number:** B0581
Presentation Time: 11:00 AM–12:45 PM
Perfused Large Vessel and Capillary Densities in Various Grades of Papilledema Using OCTA Custom Software
David Fell[1, 2], Sherief Raouf[1, 2], Toco Y. Chui[1, 3], Patricia M. Garcia[1], Shelley Mo[1, 4], Sarita B. Dave[1], Nicole K. Scripsema[1, 3], Richard B. Rosen[1, 3], Rudrani Banik[1, 3]. [1]Ophthalmology, New York Eye and Ear Infirmary of Mount Sinai, New York, NY; [2]Medicine, Stony Brook University School of Medicine, Stony Brook, NY; [3]Ophthalmology, Icahn School of Medicine at Mount Sinai, New York, NY; [4]Medicine, Icahn School of Medicine at Mount Sinai, New York, NY.
Purpose: Optical Coherence Tomography Angiography (OCTA) Angioanalytics™ software has limitations in papilledema including: inaccurate autosegmentation, difficulty identifying the scleral canal border and inability to separate large vessels (LV) from capillaries. The purpose of this study was to apply customized software to overcome these issues and analyze perfused vessel density in various grades of papilledema.
Methods: We performed a prospective cross-sectional analysis of eyes with papilledema using the RTVue XR Avanti™ OCTA. Images of choroid, radial peripapillary capillary (RPC), nerve head (NH), and vitreous layers were exported to MATLAB®. The choroid image was used to center a 1.95-millimeter annular ring on the scleral canal opening, and a surrounding 0.75-millimeter peripapillary ring was analyzed. Custom digital subtraction analysis software separated LVs from capillaries and calculated mean perfused LV density (PLVD) and perfused capillary density (PCD) in RPC, NH, and vitreous layers. ANOVAs comparing the results of each layer by papilledema

grade were performed, with post-hoc Tukey's procedure (PHTP) to examine individual relationships.
Results: One eye from each of 56 subjects with papilledema, Frisén grades 0-5 and atrophic papilledema (n = 7, 14, 15, 4, 5, 2, and 9, respectively), was analyzed. ANOVA with LV subtraction analysis revealed significant changes in PCD throughout all three layers (P≤0.04). PHTP showed patterns of decreased PCD in high grade and atrophic papilledema compared to low grade. ANOVA of LV analysis showed significant changes in PLVD within the NH (P=.01) and vitreous (P=0.002) layers. PHTP showed decreased PLVD in high grades within the NH layer and increased PLVD in atrophic subjects within the vitreous layer, when compared to low grade papilledema.
Conclusions: Customized OCTA post-processing software demonstrated significantly decreased PCD across high-grade papilledema and post-papilledema optic atrophy. LV analysis of NH and vitreous layers may reflect changes in LV visibility secondary to changes in peripapillary retinal nerve fiber layer thickness.

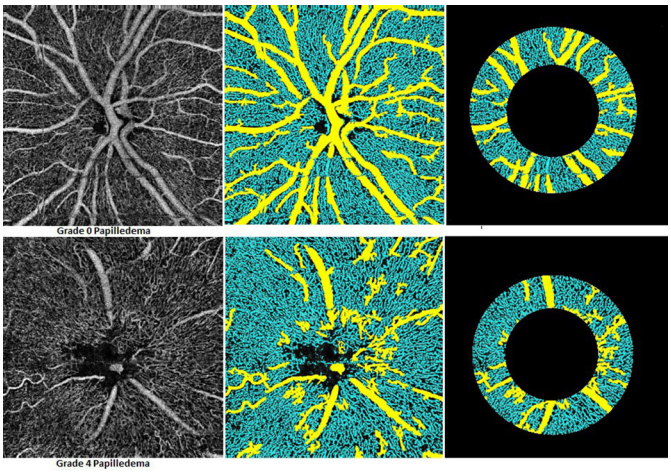

NH Layer - (Left to right) Original OCTA image, OCTA image with vessel separation, and isolated peripapillary ring in low grade (0) and high grade (4) papilledema.
Commercial Relationships: David Fell, None; **Sherief Raouf**, None; **Toco Y. Chui**, None; **Patricia M. Garcia**, None; **Shelley Mo**, None; **Sarita B. Dave**, None; **Nicole K. Scripsema**, None; **Richard B. Rosen**, Optovue (C); **Rudrani Banik**, None

Program Number: 3306 **Poster Board Number:** B0582
Presentation Time: 11:00 AM–12:45 PM
Fractal Analysis of Peripapillary Vasculature In Eyes With Papilledema Using Optical Coherence Tomography Angiography
Soshian Sarrafpour[1], Edmund Tsui[1], David Fell[2, 3], Sherief Raouf[2, 3], Nicole K. Scripsema[2, 4], Sarwar Zahid[1], Sarita B. Dave[2], Patricia M. Garcia[2], Toco Y. Chui[2, 4], Richard B. Rosen[2, 4], Rudrani Banik[2, 4], Joshua A. Young[1]. [1]Ophthalmology, New York University, New York, NY; [2]Ophthalmology, New York Eye and Ear Infirmary of Mount Sinai, New York, NY; [3]Stony Brook University School of Medicine, Stony Brook, NY; [4]Icahn School of Medicine at Mount Sinai, New York, NY.
Purpose: To quantify the fractal dimension (FD) of eyes with papilledema as compared with control eyes using Optical Coherence Tomography Angiography (OCTA).
Methods: A retrospective study was performed in 49 eyes with papilledema and 40 control eyes. OCTA images were obtained using the RTVue XR Avanti (Optovue Inc., Fremont, CA, USA). Peripapillary scans of 4.5mm x 4.5mm diameter were obtained. Grayscale OCTA images were standardized and binarized using ImageJ (National Institutes of Health, Bethesda, Maryland, USA). Fractal box-counting analyses were performed using Fractalyse (ThéMA, Besançon Cedex, France). Statistical analysis was performed using one-way analysis of variance with post-hoc Tukey's multiple comparisons test and two-tailed t-test. Further analyses were performed on papilledema subgroups based on severity (Grade 0, n=12; Grade 1, n=15; Grade 2, n=13; Grade 3, n=5; Grade 4/5, n=4).
Results: The mean FD of all eyes with papilledema (1.677, SD=0.075) was significantly higher (P=0.0021) than control eyes (1.630, SD=0.062). The FD in papilledema subgroups based on severity were Grade 0 (1.707, SD=0.047), Grade 1 (1.675, SD=0.046), Grade 2 (1.674, SD=0.090), Grade 3 (1.610, SD=0.139), Grade 4/5 (1.694, SD=0.060). Analyses between papilledema subgroups demonstrated a significant increase (P<0.05) in FD between Grade 0 papilledema and control eyes. There were no significant differences in pairwise comparisons between other subgroups.
Conclusions: The FD in OCTA of eyes with papilledema was significantly higher compared to control eyes. When analyzed by severity, eyes with Grade 0 papilledema had a higher FD compared to control eyes. Since fractal geometry reflects the branching of the peripapillary microvasculature, an increased FD may correlate with an increase in perfused vessel density as identified by OCTA. Fractal analysis in OCTA has the potential to establish quantitative parameters for peripapillary microvascular pathology in papilledema.
Commercial Relationships: Soshian Sarrafpour, None; **Edmund Tsui**, None; **David Fell**, None; **Sherief Raouf**, None; **Nicole K. Scripsema**, None; **Sarwar Zahid**, None; **Sarita B. Dave**, None; **Patricia M. Garcia**, None; **Toco Y. Chui**, None; **Richard B. Rosen**, Optovue (C); **Rudrani Banik**, None; **Joshua A. Young**, None

Program Number: 3307 **Poster Board Number:** B0583
Presentation Time: 11:00 AM–12:45 PM
Characteristics and Incidence of Inpatient Ophthalmology Consultations to Screen for Papilledema
Peter J. Belin, Giovanni Greaves, Alexander Weiss, Jules Winokur, Matthew Gorski. Ophthalmology, Hofstra Northwell School of Medicine, Great Neck, NY.
Purpose: Ophthalmology consultation is common in the inpatient and emergency room setting to "rule out papilledema" in cases of headache, blurry vision, head trauma, intracranial mass, or elevated intracranial pressure. The purpose of this study is to evaluate the incidence of ophthalmology consultations to screen for papilledema in an acute inpatient setting and determine the frequency and factors associated with a positive diagnosis of bilateral optic nerve swelling.
Methods: A retrospective chart review was performed of consecutive adult and pediatric inpatient ophthalmology consultations to "rule out papilledema" from September through November 2016. All patients had a detailed neuro-ophthalmology examination including a dilated fundus exam.
Results: A total of 28 consults—11 males and 17 females—with a mean age of 17 (range 3-71) were called to screen for papilledema. The most common service to request the consult was pediatrics (50%), followed by neurosurgery (32%), medicine (11%), and neurology (7%). The most frequent reason for consultation was headache (57%), followed by visual changes (25%) and nausea/vomiting (21%) (Table 1). A positive diagnosis of bilateral optic nerve swelling occurred in 17.9% (5/28) of consults (Table 2). Of these five consults, four of them were sent into the hospital by an ophthalmologist who noted the bilateral optic nerve swelling and one was noted by an emergency room pediatrician. All except one had corrected near visual acuity of 20/30 or better and none had an

afferent papillary defect. Color vision was full in two of the patients, decreased in one patient, and unreliable in two patients.

Conclusions: No new cases of bilateral optic nerve swelling were found in screening consults to "rule out papilledema" in our study. All of the positive diagnoses in our study had been previously identified by another physician and known to the primary team prior to ophthalmology consultation. There were no significant associations of subjective complaints or objective findings in patients with optic nerve swelling. Further larger studies must assess the cost effectiveness and utility of screening inpatient eye exams for papilledema.

Table 1.

	N
Total	28
Average age	17.2 years (range 3-71)
Gender	11/28 (39%) Male
Consult requested by:	
- **Pediatrics**	14 (50%)
- **Medicine**	3 (11%)
- **Neurosurgery**	9 (32%)
- **Neurology**	2 (7%)
Presenting symptoms:	
- **Visual changes**	7 (25%)
- **Headache**	16 (57%)
- **Nausea or Vomiting**	6 (21%)
Bilateral optic nerve swelling	5 (17.9%)
Referred by outside ophthalmology	4 (14%)

Table 2.

Case	Age, Gender	Symptom	Ophtho Referred	Visual Acuity	Color (Ishihara)	APD	Final Dx
1	13, F	Dilated pupil, restricted extraocular motility	N	20/20 OU	12/12 OU	N	Pineal germinoma
2	13, F	Headache, nausea, vomiting	Y	20/20 OU	12/12 OU	N	Viral meningitis
3	28, F	Headache, blurry vision	Y	20/400, 20/20	Poor vision, 12/12	Unable	Atypical meningioma
4	10, M	Craniosynostosis screening exam	Y	20/30 OU	NA	N	Elevated intracranial pressure
5	25, F	Blurry vision, tinnitus	Y	20/20 OU	12/12 OU	N	Idiopathic intracranial hypertension

Commercial Relationships: Peter J. Belin, None; **Giovanni Greaves**; **Alexander Weiss**, None; **Jules Winokur**, None; **Matthew Gorski**, None

Program Number: 3308 **Poster Board Number:** B0584
Presentation Time: 11:00 AM–12:45 PM

Objective Quantification of Papilledema Resolution after Optic Nerve Sheath Fenestration

Steven E. Katz[1, 2], Ashraf M. Mahmoud[2, 3], Cynthia J. Roberts[2, 3].
[1]Ophthalmology, Ohio ENT, Columbus, OH; [2]Ophthalmology & Visual Science, The Ohio State University, Columbus, OH; [3]Biomedical Engineering, The Ohio State University, Columbus, OH.

Purpose: To objectively quantify change in papilledema after optic nerve sheath fenestration (ONSF) using optical coherence tomography (OCT) in Idiopathic intracranial hypertension (IIH).

Methods: Twenty-four eyes of 12 subjects diagnosed with IIH were prospectively enrolled to investigate changes in nerve head morphology using OCT after bilateral ONSF. The central line of HD 5 Line Raster exams using a Cirrus HD-OCT were acquired pre-operatively, at one day and at one month post-operatively. Papilledema height (PapH) was quantified by connecting Bruch's membrane opening with a linear segment, and generating a normal segment from this reference line to the maximum height of the nerve head. (Figures 1 and 2) The x and y dimensions of the height segment were scaled and converted to mm based on scan parameters. Images of poor quality were excluded. Paired T-tests were performed between pre-op and 1 day post-op, as well as between 1 day and 1 month post-op. Significance threshold was $p < .05$. In addition, linear regression analysis was performed between PapH and subjective estimate of papilledema graded by modified Frisén score for validation.

Results: Three eyes of two subjects were excluded, resulting in 21 eyes of 11 subjects at one day and 16 eyes of 9 subjects at one month post-op. A significant reduction in PapH was found between pre-op (1.14 ± .37mm) and 1 day (0.92 ± .25mm; $p < .001$), as well as between 1 day (0.93 ± .28mm) and 1 month (0.74 ± .23mm; $p < .001$). A significant relationship was found between PapH and subjective estimate by modified Frisén score ($R^2 = .4450$, $p < .0001$).

Conclusions: Optic nerve sheath fenestration allows rapid resolution of papilledema in IIH subjects, with significant reduction at one day post-operatively using objective evaluation of OCT images. Future studies will involve quantification of volume of papilledema.

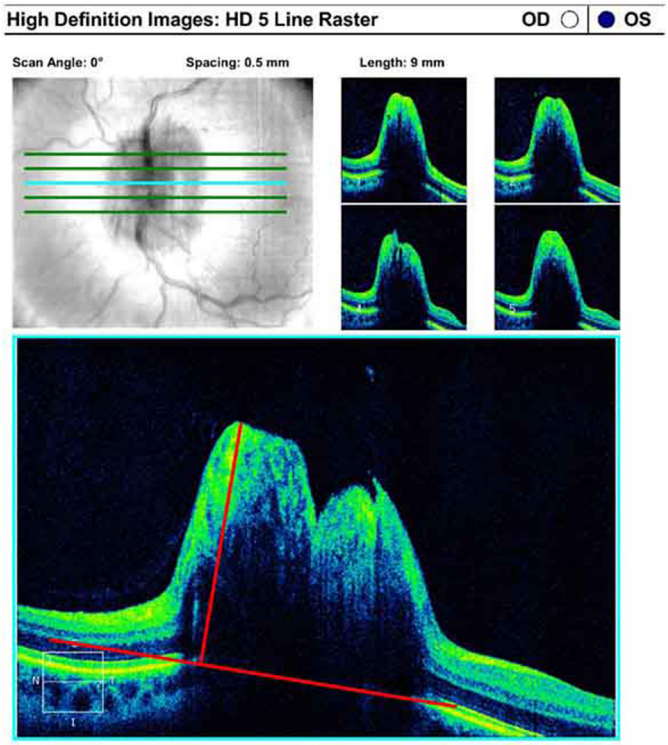

Pre-operative OCT image

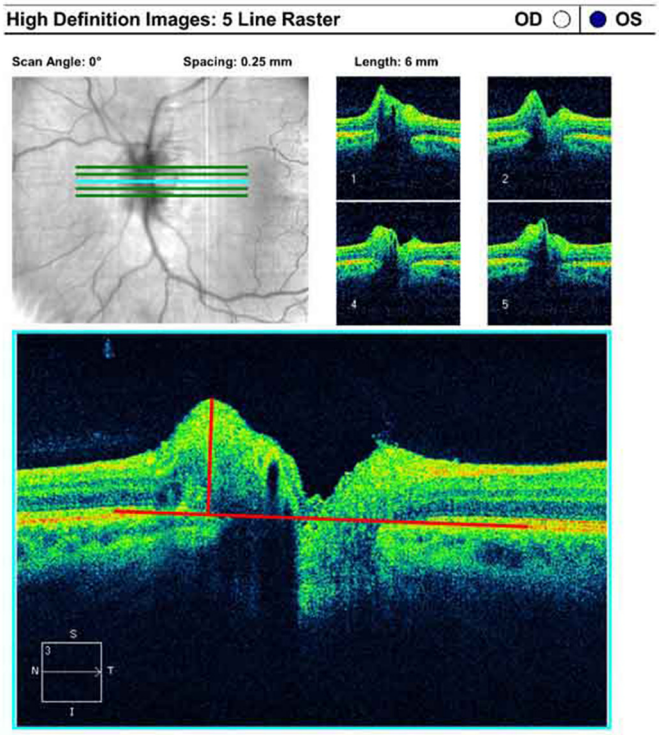

1 month post-operative OCT image
Commercial Relationships: Steven E. Katz, None; **Ashraf M. Mahmoud**, None; **Cynthia J. Roberts**, Optimeyes (C), Oculus (C), Ziemer (C)

Program Number: 3309 **Poster Board Number:** B0585
Presentation Time: 11:00 AM–12:45 PM
Hodgkin's Lymphoma Masquerading As Intermediate Uveitis And Bilateral Optic Disc Edema
Mindy Wang, Fouad El Sayyad, Hazem Samy. Ophthalmology, University of Florida, Gainesville, FL.
Purpose: While previous case reports have documented Hodgkin's lymphoma patients to have granulomatous posterior uveitis, periphlebitis, focal chorioretinitis, and vitritis, we present a case that uniquely presents with bilateral optic disc edema and intermediate uveitis in addition to retinal vasculitis on intravenous fluorescein angiography prior to diagnosis of Hodgkin's lymphoma.
Methods: A 55 year old patient presents with complaints of floaters in the left eye and blurry vision. She was found to have bilateral disc edema and intermediate uveitis in the left eye. She also had retinal vasculitis on intravenous fluorescein angiography. Following a comprehensive work-up, her axillary lymph node excisional biopsy showed classical Hodgkin Lymphoma of mixed cellularity type, diagnosing her with stage 3 Hodgkin's disease. She was started on the ABVD chemotherapy regimen and has been in remission following its completion. Her intermediate uveitis and bilateral disc edema resolved following chemotherapy treatment.
Results: Hodgkin's lymphoma can present with intermediate uveitis and bilateral optic disc edema. These ocular findings can resolve following appropriate treatment of Hodgkin's lymphoma.
Conclusions: It is essential to consider that Hodgkin's lymphoma may initially present with ocular impairment, and that one should have a high index of suspicion to promptly diagnose and treat the masquerading syndrome. Hodgkin's lymphoma should be considered in the differential diagnosis when a patient presents with unexplained disc edema with uveitis.
Commercial Relationships: Mindy Wang, None; **Fouad El Sayyad**, None; **Hazem Samy**, None

Program Number: 3310 **Poster Board Number:** B0586
Presentation Time: 11:00 AM–12:45 PM
Advances in imaging of Optic Disc Edema : Role of Oximetry and its relation with visual feild defects
NEHA SUDHAKAR S. PERAKA[1], Abdul Rawoof[2], Naresh K. Yadav[1], Rohit Shetty[3], Ashwin Mohan[1]. [1]Vitreoretina, Narayana Nethralaya, Bangalore, India; [2]Neurophthalmology, Narayana nethralaya, Bangalore, India; [3]Cornea and Refractive Surgery, Narayana Nethralaya, Bangalore, India.
Purpose:
To determine role of oximetry in calculating oxygen saturation in cases with optic disc edema and establishing correlation with visual field defects
Methods: Twenty consecutive eyes diagnosed to have disc edema secondary to various pathologies diagnosed on basis of clinical examination underwent non-invasive dual wavelength photo-spectrometric imaging of the retina (Oxymap T1, Oxymap hf, Reykjavik, Iceland) to determine the oxygen saturation in the retinal vessels and their diameters. They also underwent standard automated perimetry on the Humphrey Field Analyzer (HFA™,Carl *Zeiss* Meditec) The retinal oximetry values obtained were compared with age matched normals and also correlated with mean deviation on automated perimetry
Results: Arteriolar diameters were reduced and venous diameters were increased in the affected eyes. Arteriolar saturations were increased, venous saturations were decreased and arterio-venous saturation difference (AVSD) was increased as compared to the age matched normals. Significant positive correlation has been noted between arteriolar saturation and mean deviation
Conclusions: Decreased arteriolar diameters and increased venous diameters suggest stasis possibly due to the increased pressure due to optic nerve head edema. This may result in increased arterio-venous transit time thus allowing more time for oxygen exchange. This could possibly explain the increased arterio-venous saturation difference. Oximetry may be useful in the screening and quantifying the imapct of disc edema on visual function in patients with disc edema
Commercial Relationships: NEHA SUDHAKAR S. PERAKA; **Abdul Rawoof**, None; **Naresh K. Yadav**, None; **Rohit Shetty**, None; **Ashwin Mohan**, None

Program Number: 3311 **Poster Board Number:** B0587
Presentation Time: 11:00 AM–12:45 PM
The Relationship between Central Corneal Thickness (CCT) and Papilledema from Idiopathic Intracranial Hypertension (IIH)
Caroline Vasseneix[2], Michael Dattilo[2], Beau B. Bruce[2, 1], Nancy J. Newman[2, 3], Valerie Biousse[2, 4], Jason Peragallo[2, 5].
[1]Department of Epidemiology, Emory University, Atlanta, GA; [2]Neuro-Ophthalmology unit, Department of Ophthalmology, Emory University, Atlanta, GA; [3]Department of Neurological surgery, Emory University, Atlanta, GA; [4]Department of Neurology, Emory University, Atlanta, GA; [5]Department of Pediatric Ophthalmology, Emory University, Atlanta, GA.
Purpose: Glaucoma studies have suggested that translaminar pressure gradients (TPG) may affect severity of optic nerve damage in glaucoma. It has been demonstrated that CCT could possibly be a risk factor for developing ophthalmic disease from an altered TPG. Alterations of TPG by decreasing intraocular pressure (IOP) have also been implicated in the development of papilledema. Subgroups

of patients with IIH and papilledema are at higher risk for severe vision loss, including black patients, men, and patients with fulminant presentations. Our goal was to determine if CCT is related to severity of papilledema and vision loss in IIH.
Methods: CCT was systematically recorded in IIH patients seen between 03/2015-10/2016. Demographic data, medications, BMI, IOP, CSF opening pressure, visual acuity, color vision, visual fields, and Frisén grade of papilledema on review of fundus photography were collected. We examined associations between CCT and other variables of interest controlling for age, race, and sex using linear, logistic, and ordinal generalized estimating equation models to account for intereye correlations.
Results: Our 100 IIH patients included 95/100 women; 35 white, 56 black, 9 other race; with a median age 31 years (IQR 24.8-36.2), median BMI 35.7 (31.1-43), and median follow up 10.7 months (1.6-20.2). Median CCT was 551µ OD (525-578) and 553µ OS (529-577). Among 142/200(71%) eyes with papilledema at presentation, 39(20%) were Frisén scale grade 1 or 2, 40(20%) grade 3, 16(8%) grade 4, and 8(4%) grade 5. Median visual acuity was 0 logMAR and 36% had a visual field defect at first and final presentation. There was no association between CCT and IOP, CSF opening pressure, BMI, severity of papilledema and final visual outcome, controlling for age, race, and sex.
Conclusions: IIH patients had a median CCT within the normal range. There was no association between CCT, IOP, or TPG and severity of papilledema or visual outcome.
Commercial Relationships: Caroline Vasseneix, None; **Michael Dattilo**, None; **Beau B. Bruce**, None; **Nancy J. Newman**, None; **Valerie Biousse**, None; **Jason Peragallo**, None
Support: Research to Prevent Blindness departmental grant (Department of Ophthalmology, Emory University), and National Eye Institute, National Institutes of Health, Bethesda, Maryland (core grant no.: P30-EY006360)

Program Number: 3312 **Poster Board Number:** B0588
Presentation Time: 11:00 AM–12:45 PM
MRI quantification of intraconal fat volume in patients with Idiopathic Intracranial Hypertension
Laurel Tainsh[1], Syed A. Hussnain[1], Amy Yuan[1], Anshu Shukla[2], Michael Ehrlich[1]. [1]Ophthalmology and Visual Science, Yale School of Medicine, New Haven, CT; [2]Radiology and Biomedical Imaging, Yale School of Medicine, New Haven, CT.
Purpose: Idiopathic intracranial hypertension (IIH) is a syndrome of increased intracranial pressure with unknown etiology that is most common in obese women of childbearing age. Methods to accurately predict the severity of visual loss on neuroimaging are lacking and measurement of intraconal fat volume in patients with IIH has not been described. We performed a retrospective chart review to estimate intraconal fat volume and its association with BMI and vision in patients with IIH.
Methods: The charts from all patients with an ICD code of IIH in epic at Yale New Haven Hospital from 2010-2015 were reviewed for this study. Patients with age ≥18 years, a lumbar puncture with opening pressure >20cm water, MRI of orbits and brain, and ophthalmic exam between 2010-2015 were included. Patients were excluded if not meeting Dandy Criteria for IIH or for incomplete data. Intraconal fat was estimated by subtracting the volume of the optic nerve from the total intraconal volume on measurements from coronal T1 weighted MRI scans. Data was analyzed via linear regression.
Results: We identified 526 patients with an ICD code for IIH. Of these, 25 patients (50 eyes) were included. Mean intraconal fat volume was 1.98 cm^3 (range 1.30 – 2.61 cm^3). Mean BMI was 38.8 kg/m^2 (range 25.3-51 kg/m^2). Vision ranged from 20/20 to light perception only. 23/25 (92%) of patients were female with average age 36 yrs (range 18-61 yrs). On linear regression analysis, there was a positive correlation between intraconal fat volume and BMI (slope=0.03 ± 0.006, R^2=0.30, p=0.0001), but no correlation between intraconal volume and BCVA.
Conclusions: Intraconal fat volume varies in patients with IIH and is positively correlated with BMI. The association between intraconal fat volume and visual outcomes remains unclear. Future work will identify patients in which measurements of intraconal fat volume might predict visual outcomes and potential benefit from early intervention.
Commercial Relationships: Laurel Tainsh, None; **Syed A. Hussnain**, None; **Amy Yuan**, None; **Anshu Shukla**, None; **Michael Ehrlich**, None
Support: Research to Prevent Blindness

Program Number: 3313 **Poster Board Number:** B0589
Presentation Time: 11:00 AM–12:45 PM
Electroretinography in idiopathic intracranial hypertension: comparison of the pattern ERG and the photopic negative response
Jason C. Park, Heather Moss, J Jason McAnany. Ophthalmology, University of Illinois at Chicago, Chicago, IL.
Purpose: To evaluate the relationship between the pattern electroretinogram (pERG) and the photopic negative response (PhNR) of the flash ERG, both measures of retinal ganglion cell (RGC) function, in patients who have idiopathic intracranial hypertension (IIH).
Methods: The pERG and PhNR were recorded from 11 IIH patients and 11 age-similar, visually-normal controls. The pERG was recorded in response to a reversing checkerboard pattern that subtended 35° of visual angle. The PhNR, which is a slow negative component that follows the b-wave of the flash ERG, was recorded in response to a long-wavelength flash presented against a short-wavelength adapting field. The PhNR was elicited by both a full-field stimulus (ffPhNR) and a focal macular stimulus (fPhNR) that had an area equivalent to the angular subtense of the pERG checkerboard. PhNR amplitude was measured from baseline and pERG amplitude was measured from the P50 peak to the N95 trough. Additionally, the 24-2 Humphrey visual field mean deviation (HVF MD) was obtained for each patient.
Results: The ffPhNR, fPhNR and pERG amplitudes were all significantly correlated for the control subjects (all $r \geq 0.84$, $p \leq 0.001$), but not the IIH patients (all $r \leq 0.54$, $p \geq 0.09$). The ffPhNR, fPhNR and pERG amplitudes were outside of the normal range in 5, 4, and 3 IIH patients, respectively. On average, the patients had amplitude reductions of the ffPhNR by 35%, fPhNR by 19%, and pERG by 7%. Only the mean ffPhNR amplitude was reduced significantly in the IIH patients compared to controls ($p = 0.012$). HVF MD was correlated significantly with log fPhNR amplitude ($r = 0.76$, $p = 0.006$), but not with log ffPhNR amplitude ($r = 0.57$, $p = 0.07$) or log pERG amplitude ($r = 0.52$, $p = 0.10$).
Conclusions: Only the mean amplitude of ffPhNR was reduced significantly in IIH patients compared to controls. This may be because full-field stimuli can capture dysfunction that is localized to the far periphery, which may be overlooked by tests that are restricted to the macula. As such, full-field measures of RGC function, such as the ffPhNR, are well suited for assessing RGC dysfunction in patients who have IIH.
Commercial Relationships: Jason C. Park; **Heather Moss**, None; **J Jason McAnany**, None

Support: National Institutes of Health Grants K12EY021475 (HM), K23EY024345 (HM), and P30EY01792 (UIC Core); an Illinois Society for the Prevention of Blindness Research Grant (HM); an unrestricted departmental grant, Sybil B. Harrington (HM) and Dolly Green (JM) Special Scholar Awards from Research to Prevent Blindness.

Program Number: 3314 **Poster Board Number:** B0590
Presentation Time: 11:00 AM–12:45 PM
Patterns of Vision Loss in Idiopathic Intracranial Hypertension: The Central vs. Peripheral Visual Field

Eric Lee[1], Ashwin Subramani[1], Robert Wanzek[1], Trina Eden[1], Luke X. Chong[3], Andrew Turpin[2], Ivan Marin-Franch[4, 5], Michael Wall[6]. [1]Carver College of Medicine, University of Iowa, Iowa City, IA; [2]University of Melbourne, Melbourne, VIC, Australia; [3]University of California at Berkeley, Berkeley, CA; [4]Departamento de Óptica y Optometría y Ciencias de la Visión, Universitat de València, Valencia, Spain; [5]Ciencias de la Visión research group, Facultad de Óptica y Optometría, Universidad de Murcia, Murcia, Spain; [6]Neurology, Ophthalmology and Visual Sciences, University of Iowa, Iowa City, IA.

Purpose: The peripheral visual field is largely unexplored with static threshold automated perimetry. We performed a cross-sectional clinical study to both characterize visual field defects and evaluate structure-function correlation in idiopathic intracranial hypertension (IIH) subjects.

Methods: 60 control subjects with normal vision were tested twice with a new perimetry test of the central and far peripheral visual field. After creating a normative database for full field perimetry from the control subjects, the 95th, 98th and 99th percentiles for abnormality were determined for those with IIH. 22 patients seeking care for IIH at the University of Iowa Hospitals and Clinics were then recruited and underwent perimetry on the full visual field. All subjects were also tested on the Cirrus Optical Coherence Tomography (OCT) machine to determine retinal nerve fiber layer (RNFL) thickness. We then 1) characterized the visual field defects found testing the full visual field, and 2) analyzed the OCT structural data alongside vision function and determined the level of structure-function correlation.

Results: The most common defects found in the peripheral visual fields were infero-temporal wedge defect (68% – see figure), infero-nasal loss (55%), and supero-nasal loss (50%). For those with infero-temporal visual field defects in the periphery (n=15), (53%) had corresponding RNFL OCT thinning of the border of the superior and nasal optic disc that sends axons to this area. None of the subjects had thinning of the supero-nasal disc sector without a corresponding infero-temporal visual field defect. Additionally, 27% of subjects had normal central visual field examinations with an abnormality in the peripheral visual field.

Conclusions: We found temporal wedge defects to be common in IIH patients, a defect that has only been rarely reported in IIH. Additionally, this particular defect showed good correlation with OCT structural data. Another important finding was that 6 of the 22 subjects (27%) had normal central visual field testing with a visual field defect present in the far periphery. Testing the largely unexplored far peripheral visual field may be important for clinically following patients with IIH.

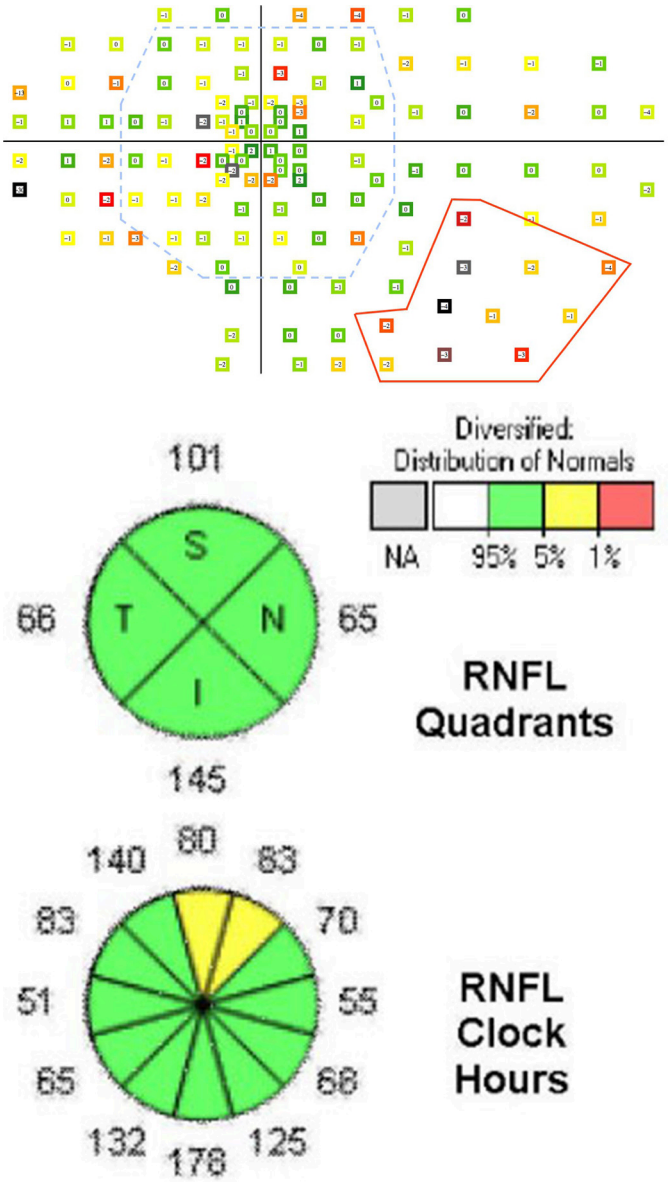

Commercial Relationships: Eric Lee, None; **Ashwin Subramani**, None; **Robert Wanzek**, None; **Trina Eden**, None; **Luke X. Chong**, None; **Andrew Turpin**, Haag-Streit (F), CenterVue (C), Heidelberg Engineering (F); **Ivan Marin-Franch**, None; **Michael Wall**, None
Support: VA Merit Review

Program Number: 3315 **Poster Board Number:** B0591
Presentation Time: 11:00 AM–12:45 PM
Detection of Visual Loss in Idiopathic Intracranial Hypertension with Static Automated Perimetry: The Far Periphery

Ashwin Subramani[1], Michael Wall[1], Eric Lee[1], Andrew Turpin[2], Luke X. Chong[3]. [1]University of Iowa, Iowa City, IA; [2]University of Melbourne, Melbourne, VIC, Australia; [3]University of California, Berkeley, CA.

Purpose: The peripheral visual field outside of the central 30° is rarely tested with static automated perimetry. We performed a cross sectional clinical study to characterize visual loss across the full visual field in idiopathic intracranial hypertension (IIH) patients.

Methods: We tested one eye of 48 controls with normal vision twice with a central and peripheral visual field exam using software

developed in our lab on the Octopus 900 perimeter running the Open Perimetry Interface (OPI). We also tested one eye of 15 IIH subjects ages 18-79 with Grade 0-1 optic disc edema with the same central and peripheral visual field exams. To compare IIH patients (mostly young women) to controls (ages spread from 20 to 70 years), we standardized all of our collected subject data to the age of 50 using linear regression. We then separated the nasal and temporal visual field data to determine the effect IIH had on both individually, then plotted sensitivity vs. centricity of both the control and IIH subjects. A Mann-Whitney Rank Sum Test was then performed to compare the best fit lines between the control and IIH data.

Results: he data shows that there is a more rapid decrease in visual sensitivity as eccentricity increases for IIH patients compared with the controls. A Mann-Whitney Rank Sum analysis was performed. In both the nasal (Fig. 1) and temporal areas of the visual field the decrease in visual sensitivity as eccentricity increased was significant ($p<0.001$).

Conclusions: We found that visual loss significantly increases with eccentricity more in IIH subjects than controls in both the nasal and temporal visual fields. Visual field testing in the far periphery has promise to show greater defects in IIH subjects compared to the central visual field.

Fig. 1. Nasal: Eccentricity vs. Sensitivity

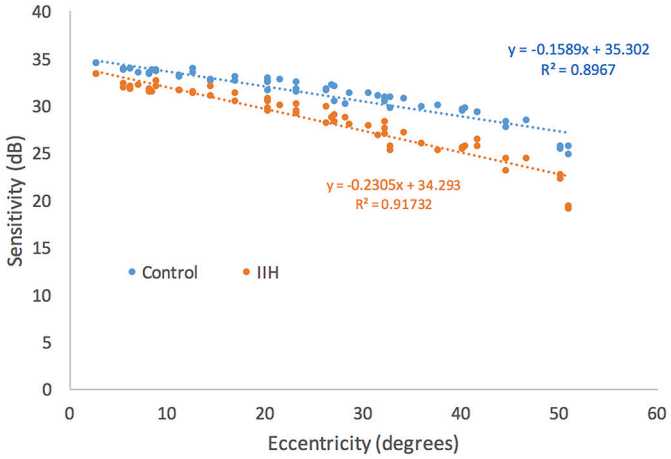

Commercial Relationships: Ashwin Subramani, None; **Michael Wall**, None; **Eric Lee**; **Andrew Turpin**, Haag-Streit (F), Heidelberg Engineering (F), GmBH (F), CenterVue SpA (C); **Luke X. Chong**, None

Support: VA Merit Review

Program Number: 3316 **Poster Board Number:** B0592
Presentation Time: 11:00 AM–12:45 PM

Treatment of Secondary Pseudotumor Cerebri from Severe Anemia with Blood Transfusion

Nehali Nanawati, Elliot Crane, Kunjal K. Modi, Roger Turbin, Larry Frohman. Department of Ophthalmology and Visual Science, Rutgers New Jersey Medical School, Newark, NJ.

Purpose: We aim to investigate blood transfusion as a treatment for patients with pseudotumor cerebri (PC) secondary to severe iron deficiency anemia.

Methods: This is a retrospective case series of three patients with PC and anemia diagnosed after lumbar puncture, neurologic imaging, and completion of extensive workup to rule out other secondary causes. Patients with pre-transfusion hemoglobin (Hb) levels less than 9 g/dl were included. Ocular and neurologic signs and symptoms of PC, as well as hemoglobin levels, were assessed on presentation and after transfusion.

Results: 3 women in their twenties with secondary PC due to severe anemia, 2 from gynecologic blood loss and 1 from pancytopenia, were identified. All patients had disc edema on presentation. Presenting hemoglobin levels were 6.2, 5.4, and 5.6 g/dl. All patients were transfused with final hemoglobin levels of 8.2, 8.9, and 10.7 g/dl, respectively (Table 1).

Case 1: 20 year-old (yo) female with heavy menstrual bleeding presented with severe headache (HA), pulsatile tinnitus (PT), and transient visual obscuration (TVO). She had an initial Hb of 6.2 and visual field (VF) changes on automated perimetry. Her BMI was 21.8. She was transfused with 2 units of red blood cells (RBC), which raised her Hb to 8.2, followed by acetazolamide. HA, PT, and TVO resolved by the following day. VA and VF also improved.

Case 2: 26 yo female with heavy menstrual bleeding presented with HA, PT, and TVO. She had an initial Hb of 5.4 and was morbidly obese (BMI = 50.2). She was treated with acetazolamide and transfused with 4 units of RBC, which raised her Hb to 8.9. HA, PT, and TVO resolved 2 days post-transfusion.

Case 3: 24 yo female with idiopathic pancytopenia presented with HA, PT, and TVO with visual loss in the right eye. Her initial Hb was 5.6 and BMI was 30.1. Fundus exam revealed Roth spots in the right eye. She was treated with high dose steroids and transfused with 4 units of RBC which raised her Hb to 10.7. Her symptoms resolved by 5 days post-transfusion; the papilledema was resolving. No other cause for the Roth spots was found.

Conclusions: All three patients with PC and severe anemia in our case series demonstrated rapid resolution of symptoms of PC (HA, PT, and TVO) after blood transfusion. In patients with PC secondary to severe anemia, anemia correction with blood transfusions may help to alleviate symptoms and obviate the need for surgical intervention.

Table 1. Changes in ocular signs and symptoms of pseudotumor cerebri after blood transfusion.

Patient	Transfusion Status (# of units of RBCs)	Hemoglobin [g/dl]	Presenting Symptoms	Visual Acuity (RE, LE)	Disc Edema Frisen Scale [grade]	Visual Fields [dB]
1	pre	6.2	HA + PT + TVO +	20/20-1, 20/25	RE: II LE: III	RE: MD -3.50, PSD 4.29 LE: MD -4.43, PSD 3.62
	1 day post (2)	8.2	HA - PT - TVO -	20/20, 20/20	n/a	n/a
2	pre	5.4	HA + PT + TVO +	20/200, 20/60-1	RE: II-III LE: II-III	n/a
	2 days post (4)	8.9	HA - PT - TVO -	20/200, 20/100	RE: II LE: II	RE: MD -21.44, PSD 8.48 LE: MD -12.72, PSD 7.90
3	pre	5.6	HA + PT + TVO +	CF @ 3', 20/40	RE: IV LE: III	RE: MD -33.36, PSD 2.60 LE: MD -7.94, PSD 8.53
	5 days post (4)	10.7	HA - PT - TVO -	20/200+1, 20/25	RE: III-IV LE: III	RE: MD -31.94, PSD 5.59 LE: MD -12.34, PSD 11.95

HA = headache, PT = pulsatile tinnitus, TVO = transient visual obscuration, CF = counting fingers, RBCs = red blood cells, RE = right eye, LE = left eye, MD = mean deviation, PSD = pattern standard deviation

Commercial Relationships: Nehali Nanawati, None; **Elliot Crane**, None; **Kunjal K. Modi**, None; **Roger Turbin**, None; **Larry Frohman**, None

Program Number: 3317 **Poster Board Number:** B0593
Presentation Time: 11:00 AM–12:45 PM

Optic nerve head geometry as a function of chronic intracranial pressure

Heather Moss[1], Kiran Malhotra[2], megh patel[3], Zainab Shirazi[2]. [1]Ophthalmology, Stanford University, Palo Alto, CA; [2]College of Medicine, University of Illinois at Chicago, Chicago, IL; [3]Department of Bioengineering, University of Illinois at Chicago, Chicago, IL.

Purpose: Chronic elevations in intracranial pressure(ICP) are associated with ophthalmic geometric changes including optic nerve head(ONH) swelling and peripapillary Bruch's membrane(BM) displacement. The objectives of this project were 1.to determine the quantitative relationship between ICP magnitude and geometric

ophthalmic features and 2.to evaluate the suitability of geometric ophthalmic features for discriminating high from normal ICP.
Methods: 6 OCT B-scans of the ONH(radial scan pattern, Spectralis, Heidelberg Engineering) were obtained in both eyes of 20 subjects(age 23-86yrs) prior to lumbar puncture(LP). ICP was measured as LP opening pressure(10-55 cm H_2O). Inner limiting membrane(ILM) and BM were manually segmented on each image by two raters. ONH volume(ONHV) was defined as tissue between ILM and BM in in a 3mm diameter circle centered on the ONH and was calculated for each eye by interpolating between images. Perpendicular distances between each of the two BM opening points and the secant line intersecting BM 2mm on either side of the ONH center were calculated for each image and summed across images to generate BM opening distance(BMOD) for each eye. Relationships between ICP and geometric features were modeled using generalized estimating equations(GEE). Area under the curve(AUC) from receiver operating characteristic analysis evaluated the ability to discriminate high(≥ 25 cm H_2O) from normal(≤ 20cm H_2O) ICP and to confirm normal ICP using geometric features.
Results: Segmentation of ILM and BM was feasible in all scans for 36 eyes(90%). ICP was linearly related to both ONHV (0.010 mm^3/cm H_2O 95%CI[0.005-0.015], p<0.0005, GEE) and BMOD (39µm into the globe/cm H_2O 95%CI[25-54], p<0.0005, GEE). The probability of correctly classifying a subject as having high ICP(AUC for high vs. normal ICP, excluding borderline ICP) was 0.98 95%CI[0.91-1.0] using ONHV and 0.87[0.73-1.0] using BMOD. The probability of correctly classifying a subject as having normal ICP (AUC for normal vs. borderline or high ICP) was 0.86[0.74-0.98] using ONHV and 0.77[0.61-0.93] using BMOD.
Conclusions: We build upon prior reports of qualitative relationships between high ICP, increased ONHV and BMOD by demonstrating a quantitative relationship between chronic ICP and ophthalmic geometric features. Distinguishing between ICP states may be possible based on geometric ophthalmic features. The basis of misclassified cases requires further study.

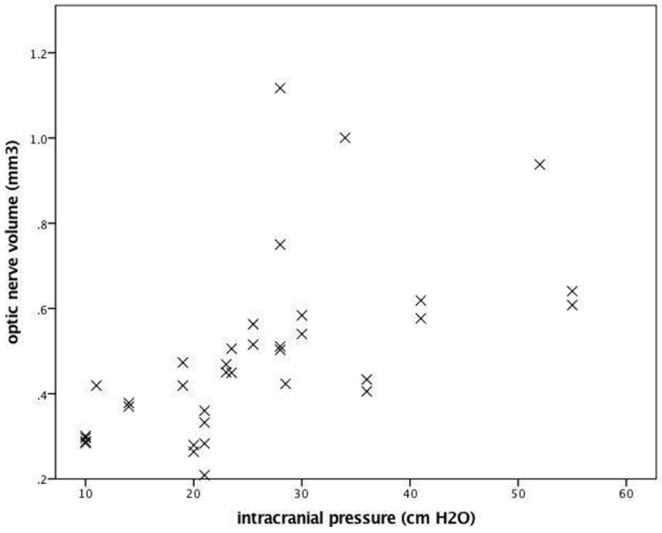

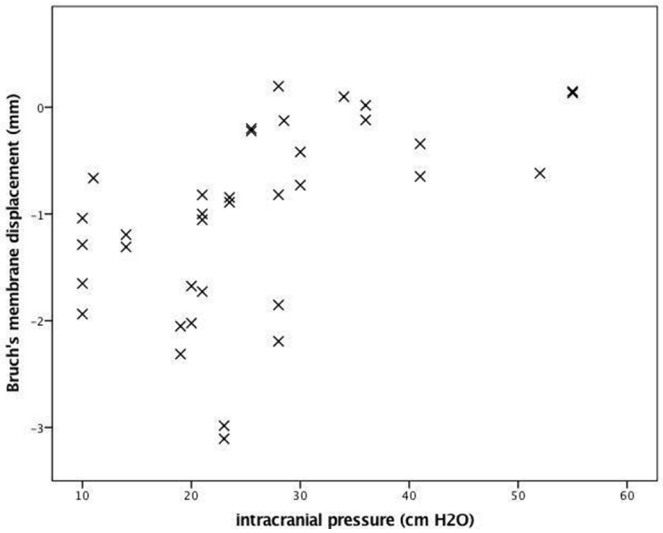

Commercial Relationships: Heather Moss, None; **Kiran Malhotra**, None; **megh patel**, None; **Zainab Shirazi**, None
Support: NIH K23-EY024345, Research to Prevent Blindness unrestricted grant & Special scholar award, Illinois Society for the Prevention of Blindness Research grant

Program Number: 3318 **Poster Board Number:** B0594
Presentation Time: 11:00 AM–12:45 PM
MR imaging of the optic nerve and chiasm at 7 Tesla improves lesion detection for Neuro-Ophthalmic conditions compared to conventional clinical field strength
Lorna Grech Fonk[1, 3], Marco Verstegen[2], Wouter Teeuwisse[3], Teresa Ferreira[3], Irene Notting[1], Wouter van Furth[2], Alberto Pereira[4], Gregorius P. Luyten[1], Andrew Webb[3], Jan-Willem Beenakker[1, 3].
[1]Ophthalmology, Leiden University Medical Centre, Leiden, Netherlands; [2]Neurosurgery, Leiden University Medical Center, Leiden, Netherlands; [3]Radiology, C.J. Gorter Center for high field MRI, Leiden University Medical Center, Leiden, Netherlands; [4]Endocrinology, Leiden University Medical Center, Leiden, Netherlands.
Purpose: Growth of a pituitary adenoma impinges on the optic chiasm causing visual field (VF) defects to varying degrees. Surgical removal of the tumor often restores most of the visual function. However, the VF defects occasionally reoccur years after successful treatment. MRI is currently an important tool for diagnosis and therapy planning. Conventional clinical scanners operate at a field strength of 3 Tesla (T). However, scanning patients at the ultra-high field strength of 7T has the potential to acquire higher resolution images than at 3T. In this study, we evaluate the additional value of 7T MRI in the diagnosis and treatment of pituitary macro-adenomas.
Methods: Nine controls and seven patients were scanned on a commercial Philips whole body 7T MR system. 3D T1-weighted gradient-echo with isotropic resolution (0.7mm^3); and 2D T2-weighted spin echo (0.45x0.45x1.0mm^3) were acquired. For comparison, standard clinical protocol was run on a 3T Philips system.
Results: The 7T scan protocol gave reproducible image quality for each of the patients scanned, with image quality superior to 3T. In three patients the 7T MRI revealed important clinical information that was not visible at 3T. In two patients, a small lesion was noted in the optic nerve (ON) at 7T (Figure 1) which was not visible in the 3T images. The location of the lesions corresponded to the VF defects. This was an important confirmation for the ophthalmologists to tailor

treatment strategy. In a second patient, the thinner (1mm vs 3mm) slices that could be acquired at 7T due to its superior signal-to-noise showed tumor contact with the chiasm (Figure 2) whilst at 3T this was not visible. This was key for the neurosurgeon to plan the best intervention.

Conclusions: This study shows that 7Tesla MRI provides direct clinical opportunities for the treatment of patients with pituitary tumors and other neuro-ophthalmic conditions.

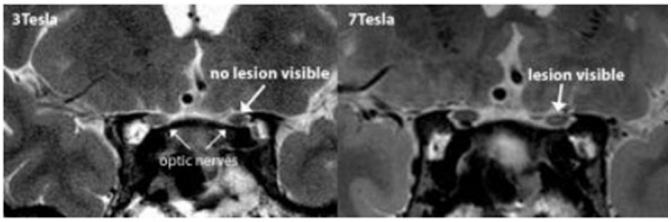

VF defect recurrence 4 years post treatment. Hyperintense lesions in ON clearly visible and not visible on 3T. Location of lesions corresponds with VF defect

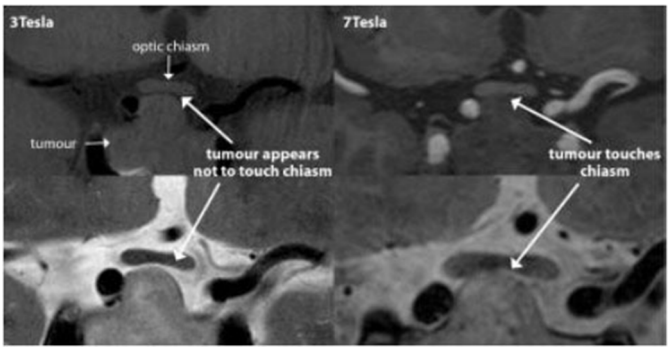

T1 (top) T2 (lower) pre-op MRI showing large pituitary macro-adenoma. 7T image shows contact between tumor and chiasm, this is not apparent on 3T

Commercial Relationships: Lorna Grech Fonk; **Marco Verstegen**, None; **Wouter Teeuwisse**, None; **Teresa Ferreira**, None; **Irene Notting**, None; **Wouter van Furth**, None; **Alberto Pereira**, None; **Gregorius P. Luyten**, None; **Andrew Webb**, None; **Jan-Willem Beenakker**, None

Program Number: 3319 **Poster Board Number:** B0595
Presentation Time: 11:00 AM–12:45 PM

Quantitative measure of optic disc drusen location in enhanced depth imaging optical coherence tomography scans

Anne-Sofie W. Lindberg[1], *Lasse Malmqvist Larsen*[2], *Vedrana Andersen Dahl*[1], *Thomas Martini Jørgensen*[1], *Steffen Ellitsgaard Hamann*[2]. [1]DTU Compute, Technical University of Denmark, Kongens Lyngby, Denmark; [2]Centre of Head and Orthopaedics - Department of Ophthalmology, Rigshospitalet - Glostrup, Glostrup, Denmark.

Purpose: A quantitative measure of anatomical optic disc drusen (ODD) location in the optic nerve head can be an important parameter in the investigation of ODD formation and the development of visual field defects. We propose a method for defining a quantitative measure of ODD location relative to Bruch's membrane.

Methods: Optic disc drusen in high resolution enhanced depth imaging optical coherence tomography scans were manually segmented using ITK-SNAP by a trained ophthalmologist. To quantify a location of each ODD, we need a reference. Bruch's membrane serves as an excellent reference, but does not exist within the optic nerve head, where the ODD are located. Therefore we performed a semi-automatic graph based segmentation of Bruch's membrane at the margin in each B-scans. From the segmentation we obtained two landmarks per B-scan. Based on the landmarks in each B-scan, we defined a reference surface relative to Bruch's membrane. The Euclidean distance from the center of mass of each manually segmented ODD to the defined reference surface gave a quantitative measurement of each druse location. Furthermore, the quantitative measure was signed which indicated whether the ODD was located above or below the reference surface.

Results: We computed a reference surface (Fig. 1) based on Bruch's membrane segmented at the margin in 97 B-scans per patient for 37 patients in total (Fig. 2). The average number of ODD was 4.4 (± 5.78) per patient and the average distance from the center of mass for each ODD to the defined reference surface was 0.19 mm (± 0.3 mm).

Conclusions: A defined reference surface based on Bruch's membrane in ODD patients resulted in a quantitative measure of ODD location. The quantitative measure indicates whether the ODD is located above or below the reference surface. The quantitative measure of anatomical ODD location can act as an important parameter in future ODD research.

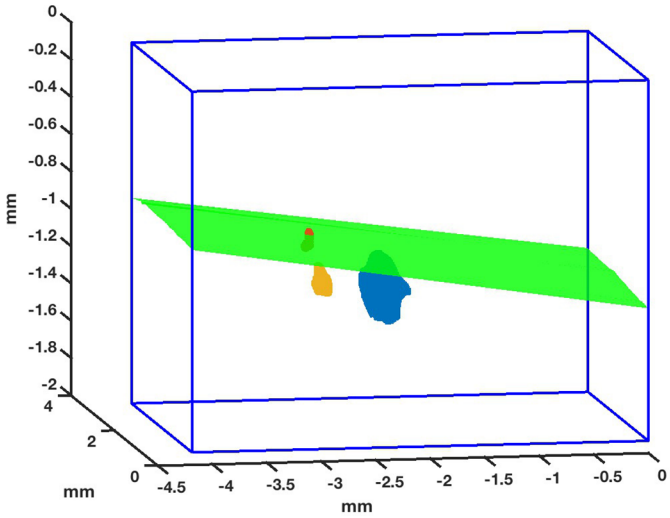

Figure 1: 3D plot of the defined reference surface (green) together with 3 optic disc drusen (red, yellow and blue). The scanned volume is indicated by the blue box.

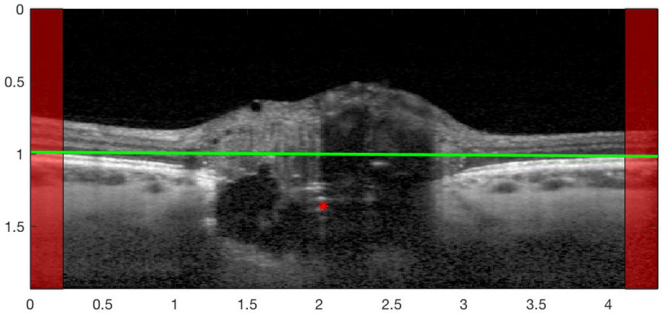

Figure 2: B-scan with the defined reference surface (green) based on a segmentation of Bruch's membrane at the margin (marked with red). The red star is the center of mass of the manual segmented druse.

Commercial Relationships: Anne-Sofie W. Lindberg; **Lasse Malmqvist Larsen**, None; **Vedrana Andersen Dahl**, None; **Thomas Martini Jørgensen**, None; **Steffen Ellitsgaard Hamann**, None

Program Number: 3320 **Poster Board Number:** B0596
Presentation Time: 11:00 AM–12:45 PM
Spectral Domain Optical Coherence Tomography Findings in Patients with Congenital Optic Nerve Hypoplasia
Yi Pang, Kelly Yin, Kelly A. Frantz. Illinois Coll of Optom, Chicago, IL.
Purpose: Cirrus spectral domain optical coherence tomography (SD-OCT) has been used successfully to measure optic disc, retinal nerve fiber layer (RNFL), and macular ganglion cells. The purpose of this study was to evaluate SD-OCT parameters in eyes with congenital optic nerve hypoplasia (CONH) compared to fellow eyes in CONH subjects and control eyes in normal subjects.
Methods: A total of 29 subjects with CONH (6-66 years old) and 64 normal subjects (6-64 years old, age and race-matched) were recruited. All CONH subjects had comprehensive eye exams prior to enrollment and were diagnosed with either unilateral or bilateral CONH, resulting in a total of 39 CONH eyes. Cirrus SD-OCT 5000 was performed on all subjects. OCT images were unobtainable in one subject with bilateral CONH (thus, 37 CONH eyes were included). Only right eye data from control subjects were used for data analysis. One-way analysis of variance was used to determine whether the OCT parameters differed among the CONH, fellow, and control eyes.
Results: OCT parameters in CONH, fellow, and control eyes are listed in Table 1. There were significant differences in all OCT parameters among the three groups, including disc area, rim area, C/D ratio, RNFL thickness, and macular ganglion cell measurements (*P* values in Table 1). Post hoc tests showed statistically significant differences in all OCT parameters between CONH and control eyes, but not between fellow and control eyes. Optic disc parameters were statistically significantly different between CONH and fellow eyes; however the difference in RNFL and macular ganglion cell measurements between CONH and fellow eyes did not reach statistical significance.
Conclusions: Abnormal Cirrus SD-OCT parameters discriminated between eyes with and without CONH. CONH eyes were characterized with smaller disc area, rim area and C/D ratio as well as reduced RNFL and macular ganglion cell thickness compared to the control eyes.

Table 1. Optical Coherence Tomography Parameters in CONH (n=37), Fellow (n = 19), and Control Eyes (n = 64)

	ONH Eyes (mean, CI)	Fellow Eyes (mean, CI)	Control Eyes (mean, CI)	*P* Value
Optic disc parameters (µm)				
Disc area (mm^2)	1.46 (1.32 -1.59)	1.74 (1.56 -1.92)	1.89 (1.80 -1.98)	<0.0001
Rim area (mm^2)	1.29 (1.16 -1.41)	1.48 (1.35 -1.62)	1.42 (1.36 -1.48)	0.03
Average C/D ratio	0.27 (0.22 -0.33)	0.37 (0.25 -0.49)	0.46 (0.41 -0.5)	<0.0001
Average RNFL thickness (µm)	86.54 (79.23 -93.85)	97.79 (87.98 -107.6)	98.14 (95.3 -100.98)	<0.01
Ganglion cell measurements (µm)				
Average	71.68 (65.63 -77.72)	78.37 (74.68 -82.06)	82.88 (80.9 -84.85)	<0.0001
Minimum	60.89 (53.25 -68.53)	73.89 (68.93 -78.86)	79.86 (77.05 -82.67)	<0.0001
Superior	75.38 (67.98 -82.78)	80.00 (75.86 -84.14)	83.69 (81.15 -86.23)	0.03
Superior nasal	72.22 (64.94 -79.49)	81.63 (78.09 -85.17)	84.44 (82.28 -86.59)	<0.0001
Inferior nasal	68.38 (60.21 -76.55)	77.68 (73.14 -82.23)	83.20 (81.20 -85.20)	<0.0001
Inferior	69.81 (62.51 -77.12)	75.00 (70.44 -79.56)	81.86 (79.88 -83.84)	<0.001
Inferior temporal	72.11 (65.87 -78.35)	76.95 (72.87 -81.03)	82.72 (80.74 -84.69)	<0.001
Superior temporal	71.57 (65.76 -77.37)	77.37 (73.65 -81.09)	80.34 (76.88 -83.81)	0.02

Commercial Relationships: Yi Pang; **Kelly Yin**, None; **Kelly A. Frantz**, None

Support: Illinois Society for Prevent Blindness

Program Number: 3321 **Poster Board Number:** B0597
Presentation Time: 11:00 AM–12:45 PM
Retinal cardiolipin metabolism is altered in a mouse model of Dominant Optic Atrophy
Emmanuelle Sarzi[1], Allel Chabli[5], Marie Seveno[1], Christian P. Hamel[1, 2], Agnes Müller[4, 1], Guy Lenaers[1, 3], Cecile Delettre[1]. [1]Inserm U1051, Institute for Neurosciences of Montpellier, Montpellier, France; [2]CHU Gui de Chauliac, Montpellier, France; [3]Inserm U1083, Angers, France; [4]Université de Montpellier, Montpellier, France; [5]Hôpital Necker Enfants Malades, Paris, France.
Purpose: *OPA1* mutations are responsible for Autosomal Dominant Optic Atrophy (ADOA), one of the most frequent hereditary optic neuropathies, characterized by retinal ganglion cell degeneration, the underlying mechanisms of which are poorly understood. We previously described the existence of a mitochondrial complex IV defect due to respiratory chain supercomplex instability in retina of the *Opa1*^{delTTAG} mouse model, contributing to ADOA pathophysiology. Thus, here we tested the hypothesis of retinal cardiolipin metabolism modification in mitochondria responsible for these respiratory chain alterations. Indeed, cardiolipins are specific phospholipids of the inner mitochondrial membrane which have a key role in the stabilization of respiratory chain supercomplexes and in particular mitochondrial complex IV.
Methods: Using the mouse model carrying the human recurrent *OPA1* mutation, we quantified in retina (n=3-5) cardiolipins and cardiolipin precursors, monolysocardiolipins (MLCL) by LC-MS/MS. Quantification of these compounds is crucial to assess the quality and efficiency of cardiolipin synthesis and remodeling.
Results: Although the total amount of cardiolipin was unchanged, we disclosed in retinal samples increased amount of the major specie of cardiolipins, i.e. cardiolipins containing 18-carbon fatty alkyl chains with two unsaturated bonds on each of them (0.213±0.015 vs 0.405±0.13). We also found a significant increase in MLCL (0.059±0.012 vs 0.100±0.009) in these retinal samples.
Conclusions: Thus, our results showed that Opa1 haploinsufficiency impacts cardiolipin metabolism in the retina. Considering that cardiolipins and MLCL amounts are modified, our results pointed to the alteration of both synthesis and remodelling of cardiolipins. In consequence, cardiolipin quality and quantity are modified in *Opa1* mouse retinas leading to mitochondrial inner membrane structural modification and promoting mitochondrial complex IV defect.
Commercial Relationships: Emmanuelle Sarzi, None; **Allel Chabli**, None; **Marie Seveno**, None; **Christian P. Hamel**, None; **Agnes Müller**, None; **Guy Lenaers**, None; **Cecile Delettre**, None

Program Number: 3322 **Poster Board Number:** B0598
Presentation Time: 11:00 AM–12:45 PM
Mechanisms of RGC Neuroprotection Mediated by ST266
Reas Sulaimankutty[1], Kimberly Dine[1], Larry R. Brown[2], Kenneth S. Shindler[1]. [1]Ophthalmology, Univ of Pennsylvania, Scheie Eye Institute, Philadelphia, PA; [2]Noveome Biotherapeutics Inc, Pittsburgh, PA.
Purpose: Optic neuritis occurs during multiple sclerosis (MS) and induces retinal ganglion cell (RGC) loss. Thus, neuroprotective therapies are needed. We previously showed that intranasally delivered ST266, the biological secretome of Amnion-derived Multipotent Progenitor cells, attenuated loss of vision and RGCs in experimental optic neuritis, but mechanisms of its actions are not

known. Potential mechanisms by which ST266 prevents RGC loss were examined in the experimental autoimmune encephalomyelitis (EAE) model of MS.
Methods: EAE was induced in C57/BL6 mice by immunization with myelin oligodendroglial glycoprotein peptide. Mice were treated daily with 6 µL intranasal PBS or ST266 beginning day 15 through sacrifice (days 22, 30 or 42). Optic nerves were stained with mitochondrial superoxide indicator MitoSOX red. Western blot analysis was performed on proteins isolated from retinas or optic nerves. ST266-mediated RGC neuroprotection was further examined in primary retinal cell cultures exposed to 5µM staurosporine ± ST266 for 24 hrs. ST266 neuroprotective effects were challenged with exposure to specific inhibitors of SIRT1 and pAKT.
Results: MitoSOX red staining showed that ST266 treatment lead to a reduction ($p<0.01$) in reactive oxygen species in EAE optic nerves on days 22 and 42. Western blot analysis showed that ST266 treated EAE mice had increased expression of SIRT1 deacetylase (day 22, $p<0.05$) and of mitochondrial coenzyme PGC1α (days 22 and 30, $p<0.05$) in the retina, as compared to PBS treated EAE mice. Retinal and optic nerve levels of mitochondrial enzyme SDHβ increased by day 30 ($p<0.05$). Levels of pAKT were also higher ($p<0.05$) in retinas of EAE mice treated with ST266 on day 30; however, phosphorylation of PDK1 was not increased. In retinal cultures, treatment with ST266 (diluted 1:20) significantly attenuated RGC loss, and co-administration of either the SIRT1 inhibitor EX527 (2µM) or pAKT inhibitor X (7µM), blocked the protective effect of ST266.
Conclusions: Increased SIRT1 expression and mitochondrial enzymes in ST266-treated EAE mice suggest ST266 stimulation of SIRT1 deacetylase activity promotes RGC survival through increased mitochondrial biogenesis and reduction of oxidative stress. In vitro studies using specific inhibitors confirm that ST266 stimulated SIRT1 and pAKT signaling mediate RGC survival. Together results demonstrate two mechanisms involved in ST266-mediated neuroprotection.
Commercial Relationships: Reas Sulaimankutty, None; **Kimberly Dine**, None; **Larry R. Brown**, Noveome Biotherapeutics, Inc (E); **Kenneth S. Shindler**, Noveome Biotherapeutics, Inc (R), Noveome Biotherapeutics, Inc (F), Noveome Biotherapeutics, Inc (C)
Support: NIH Grant EY019014; Research to Prevent Blindness; and the F. M. Kirby Foundation

Program Number: 3323 **Poster Board Number:** B0599
Presentation Time: 11:00 AM–12:45 PM
Tissue engineered 3D cultures of meningothelial cells to study the optic nerve microenvironment during conditions of optic nerve compartmentalization
Corina Kohler[2], Laura Power[2, 4], Nauke Zeleny[1], Albert Neutzner[2], Hendrik P. Scholl[3], Peter Meyer[3], David Wendt[2, 4], Hanspeter E. Killer[1]. [1]Kantonsspital Aarau AG, Aarau, Switzerland; [2]Department of Biomedicine, University of Basel, Basel, Switzerland; [3]Department of Ophthalmology, University of Basel, Basel, Switzerland; [4]Department of Surgery, University of Basel, Basel, Switzerland.
Purpose: As a major component of the optic nerve microenvironment (ONM), meningothelial cells (MECs) cover the arachnoid, the pia and the inner wall of the dura mater as well as the trabeculae and septae within the subarachnoid space (SAS) of the brain and the optic nerve. These cells play a central role in the maintenance of cerebrospinal fluid (CSF) homeostasis and in physiological and pathophysiological processes within the SAS. To study the role of MECs, more advanced and physiologically relevant models which account for the intricate three-dimensional architecture of the SAS and the factors influencing this delicate microenvironment are required. Therefore, we developed a perfusion bioreactor-based 3D model using primary human MECs to mimic the ONM. We employ this model to study the function of MECs during optic nerve compartmentalization (ONC), a syndrome characterized by impaired CSF flow within the optic nerve SAS and linked to normal tension glaucoma and idiopathic intracranial hypertension.
Methods: Primary human MECs were seeded into a 3D porous collagen scaffold within a U-CUP perfusion bioreactor (Cellec Biotek) and cultured for 72 hours under physiological flow conditions (0.3 mm/s) to generate a meningothelial like tissue. Using immunohistochemistry, engineered ONM were compared to human samples in terms of marker protein expression. As MECs have previously been shown to act as phagocytes, functionality of MECs was assessed measuring phagocytotic activity. In addition, the response of MECs to conditions of pathophysiological flow dynamics in the ONM (0.01 mm/s) are being analysed.
Results: After 3 days of culture MECs proliferated, lining the entire scaffold. Our 3D model of the ONM revealed comparable histological characteristics to the human meningothelial cell layer of the SAS with regards to cell-cell interaction markers for gap-junctions, tight- junctions and desmosomes, thus closely resembling the *in vivo* situation. Functionally, MECs in 3D culture displayed strong phagocytotic activity as observed previously under standard culture conditions.
Conclusions: This novel perfusion bioreactor based 3D model of the ONM closely imitates the *in vivo* microenvironment of the optic nerve, making it an ideal *in vitro* model for studying fundamental aspects of MEC function and the role of MECs in ONC under physiologically relevant conditions.
Commercial Relationships: Corina Kohler; **Laura Power**, None; **Nauke Zeleny**, None; **Albert Neutzner**, None; **Hendrik P. Scholl**, Gerson Lehrman Group (C), Daiichi Sankyo, Inc. (C), Vision Medicines, Inc. (C), Acucela Inc. (F), Gensight Biologics (C), QLT, Inc. (F), Genzyme Corp./Sanofi (R), NightstaRx Ltd. (F), Guidepoint (C), Boehringer Ingelheim Pharma GmbH & Co. KG (C), ReNeuron Group Plc/Ora Inc. (R), Genentech Inc./F. Hoffmann-La Roche Ltd. (R), Intellia Therapeutics, Inc. (C), Shire (C); **Peter Meyer**, None; **David Wendt**, Cellec Biotek (C); **Hanspeter E. Killer**, None
Support: Forschungsfonds Kantonsspital Aarau

Program Number: 3324 **Poster Board Number:** B0600
Presentation Time: 11:00 AM–12:45 PM
Decellularization of Porcine and Primate Optic Nerve Lamina towards Cell Culture with Neural Progenitor Cells
Lilangi S. Ediriwickrema[1], Rebecca Fawcett[2], Neil R. Miller[1], Steven L. Bernstein[2]. [1]Ophthalmology, Johns Hopkins University, Wilmer Eye Institute, BALTIMORE, MD; [2]Ophthalmology, University of Maryland School of Medicine, Baltimore, MD.
Purpose: The optic nerve lamina cribrosa is a mesh-like collagenous structure consisting of an extracellular matrix with varying porosity and glial cell distribution through which axons of retinal ganglion cells travel en route to the lateral geniculate nucleus. There has been significant interest in its structure with respect to its possible role in the pathophysiology of glaucomatous optic neuropathy. Our goal was to evaluate decellularized porcine and primate lamina as three-dimensional matrices for stem cell growth, regeneration, and delivery.
Methods: Optic nerve laminae were dissected from porcine and primate cadaveric enucleations. The tissue specimens were embedded into a sugar moiety and subsequently sectioned into variable thicknesses using a cryotome. They were then decellularized using a chemical detergent buffer (Tris-SDS-EDTA) over several pre-determined time-points. Electron microscopy and histological

analysis using Gömöri trichrome staining confirmed complete decellularization. Select decellularized scaffolds were then sterilized, seeded with either squamous cell carcinoma cells (SCC) or human neural progenitor cells, and maintained in stem cell culture.
Results: Gömöri trichrome staining confirmed that porcine or primate optic nerve lamina sectioned at 50 µm, 100 µm, or 180 µm thicknesses were completely decellularized at 45 minutes, 1 hour, or 2 hours, respectively. Sterilized porcine laminar sections tolerated SCC and neural progenitor cell adhesion, survival, and three-dimensional growth in culture, confirming biocompatibility.
Conclusions: Chemical detergent buffer immersion results in complete decellularization of porcine and primate optic nerve lamina. These porous extracellular matrices may have a potential role as a scaffold for cellular growth and neural regeneration in treating optic neuropathy.

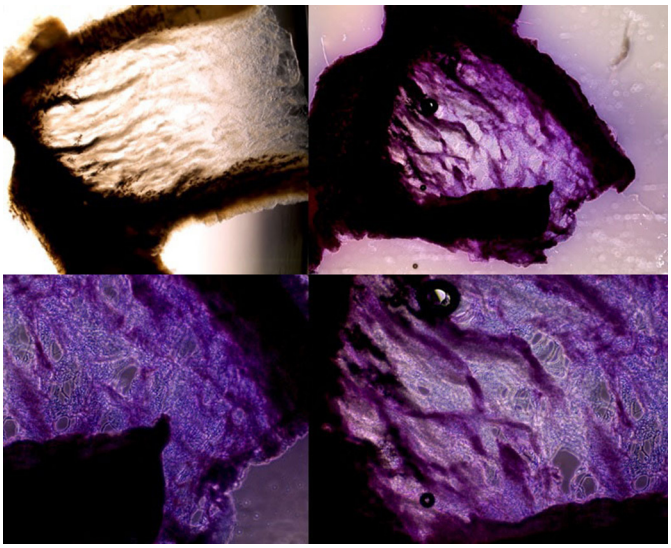

Figure 1. Decellularization of the Porcine Optic Nerve Lamina
Commercial Relationships: Lilangi S. Ediriwickrema; **Rebecca Fawcett**, None; **Neil R. Miller**, None; **Steven L. Bernstein**, None
Support: Johns Hopkins University School of Medicine, Wilmer Eye Institute Research Grant, Neuro-ophthalmology Division, 2016-7.

Program Number: 3325 **Poster Board Number:** B0601
Presentation Time: 11:00 AM–12:45 PM
Mutation analysis of CDKN2A, MYB, MYBL1 and FGFR1 in pediatric low grade gliomas of the optic pathway
Shirel Weiss[1, 2], Helen Toledano[3, 2], Orit Barinfeld[2, 1], Shalom Michowiz[4], Nitza Goldenberg-Cohen[2, 5]. [1]Sackler Faculty of Medicine, Tel Aviv University, Tel Aviv, Israel; [2]Krieger Eye Research Laboratory, Felsenstein Medical Research Center, Petach Tikva, Israel; [3]Department of Pdeiatric Oncology, Schneider Children's Medical Center of Israel, Israel, Petach Tikva, Israel; [4]Department of Neurosurgery, Schneider Children's Medical Center of Israel, Israel, Petach Tikva, Israel; [5]Ophthalmology Department, Bnai Zion Medical Center, Haifa, Israel.
Purpose: Gliomas are the commonest type of brain tumors in children. The molecular mechanisms that underlie the development and progression of these tumors are as yet unclear. A better understanding of the molecular mechanisms may improve diagnosis and treatment. In this study we investigate pediatric low grade gliomas for specific mutations in IDH1, IDH2, CDKN2A, MYB, MYBL1 and FGFR1.
Methods: 60 LGG were collected according to institutional and national IRB approval. DNA and RNA were extracted. To detect deletion in CDKN2A and mutations in MYB and MYBL-1, PCR and RT- PCR were performed. RNA seq was performed for 5 grade II and one grade I samples.
Results: CDKN2A deletions in exon 1 and exon 2 were detected in one PXA sample only.
Analysis of the MYB gene revealed 4/9 translocations with exon 2 and 4/9 translocations with exon 3 of the PCDHGA1 gene. Analysis of MYBL -1 showed 6 samples with genetic re-arrangement.
Conclusions: Mutations in MYB, MYBL and FGFR1 genes were recently reported to characterize diffuse grade 2 gliomas but not grade I gliomas. We optimized methods for analyzing gene variations and correlated to pathological grade and prognosis. We compared DNA, RNA and RNA seq results for fusion, translocation and mutations. More accurate identification of the underlying biology of different gliomas and optic pathway gliomas may pave the way for personalized medicine. This will enable targeted treatment and more accurate classification.
Commercial Relationships: Shirel Weiss, None; **Helen Toledano**, None; **Orit Barinfeld**, None; **Shalom Michowiz**, None; **Nitza Goldenberg-Cohen**, None
Support: Eshkol grant for pesenolized medicine by Minstry of Science, Technology and Space, Israel. the Zanvyl and Isabelle Krieger Fund, Baltimore, MD

Program Number: 3326 **Poster Board Number:** B0602
Presentation Time: 11:00 AM–12:45 PM
Zebrafish *rere* mutants exhibit optic nerve defects
James Liu, Aman George, Brian P. Brooks. Ophthalmic Genetics and Visual Function Branch, National Eye institute/National Institutes of Health, Bethesda, MD.
Purpose: Human patients with the *RERE* gene mutation have been reported to display autism, coloboma, optic nerve and cerebral visual defects. In mouse models, *Rere* acts as a transcriptional co-repressor to regulate *Shh* signaling and *Fgf8* expression from anterior signaling centers during embryonic development. *Rere* mRNA is expressed in developing mouse and zebrafish eyes and its loss of function is associated with microphthalmia.
Methods: To investigate the role of *rere* in optic nerve formation, we used zebrafish *rere* mutants (bab^{tb210}). Heterozygous *rere* mutant zebrafish were crossed with zebrafish expressing ath5:GFP, and then inbreed to generate homozygous *rere* mutants expressing ath5:GFP. Retinotectal projections were studied by injecting lipophilic fluorescent dyes in neural retina followed by confocal microscopy. Whole mount *in situ* hybridization was performed to study the changes in gene expression pattern.
Results: Homozygous *rere* mutant embryos expressing ath5:GFP exhibit delayed optic nerve formation and axonal path finding errors by pioneer retinal ganglion cells as studies by time lapse confocal microscopy. At 48 hours post fertilization (hpf) we could observe patterning defects in retinal ganglion cell layer and thickened hypoplastic optic nerves in homozygous *rere* mutants as compared to wild type. Some of the optic nerve fibers failed to cross the midline at optic chiasm and projected to the ipsilateral optic tectum. Defects were mainly observed in the optic nerve fibers originating from the ventro-temporal neural retina as compared to the dorso-nasal side. The amount of optic nerve fibers reaching the optic tectum was also found to be significantly reduced, as measured by calculating the fluorescently labelled surface area of the optic tectum. At the molecular level we observed a significant reduction in the expression of retinal ganglion cell markers *isl1* and *cxcr4b* at 32 and 48 hrs post fertilization. Expression of chemokine *semaphorin3d* and *slit2* was

significantly reduced in the preoptic area of *rere* mutant embryos as compared to wild type, whereas *pax2, fgf8, cxcl12a* and *netrin1* expression was expanded in the optic stalk.
Conclusions: Our study suggests that zebrafish *rere* plays an important role in establishment of visual function pathway by regulating proper pattering of the optic stalk.
Commercial Relationships: James Liu, None; **Aman George**, None; **Brian P. Brooks**, None

Program Number: 3327 **Poster Board Number:** B0603
Presentation Time: 11:00 AM–12:45 PM
T CELL MEDIATED AUTOIMMUNE TARGETING OF THE ASTROCYTIC ENDFOOT PROTEIN AQP4 LEADS TO NEURONAL/AXONAL SWELLING BUT NOT CELL LOSS IN THE RETINA
Andrés Cruz-Herranz, Sharon A. Sagan, Ryan Winger, Garrett M. Timmons, Nicholas S. Baker, Michael P. Devereux, Marc H. Levin, Collin M. Spencer, Scott S. Zamvil, Ari J. Green. Neurology, University of California San Francisco, San Francisco, CA.
Purpose: Glial cells constitute a majority of cells of the CNS and play a significant supportive role in maintaining neuronal function and survival. Targeted autoimmune mediated injury of different glial populations appears to result in different clinical disease phenotypes. While targeting oligodendrocytes via MOG results in neuronal loss, we describe here the surprising reversible pattern of injury seen with targeting AQP4 which is found on the astrocytic end feet surrounding vascular endothelium.
Methods: We induced optic nerve (ON) inflammation in female C57Bl/6J wild-type (WT) recipient mice by Th17-polarized AQP4 p201-220-specific (n=5) or MOG p35-55-specific T cells (n=5), using 5 sham-immunized mice as controls. We monitored and compared clinical severity scores and inner retinal layer (IRL) thickness obtained from Spectral Domain OCT volume scans throughout the course of disease. ONs from representative mice of all groups were stained for inflammation, demyelination, and neuronal/axonal injury. After two weeks, ganglion cells (GC) on retinal whole-mount were stained for Brn3a and quantified.
Results: All AQP4 and MOG-immunized mice developed paralysis. Onset of disease induced by AQP4 p201-220-specific T cells occurred earlier and, in contrast with EAE induced by WT MOG-specific T cells, recovery was complete. In AQP4-immunized mice, IRL thickness increased parallel to the clinical disease course, with complete return of IRL thickness to baseline upon recovery. Retinal whole-mount staining demonstrated preservation of GC. In contrast, mice that received MOG-specific T cells exhibited persistent clinical disease, which was associated with progressive IRL thinning (66±0.53 vs. 72±1.04 μm in controls at day 14, P<0.001) and loss of GC (1,847±157 vs. 4,292±110 GC/mm^2, P<0.001). AQP4-specific T cells caused ON inflammation characterized primarily as a perineuritis. In contrast, MOG-specific T cells induced severe optic neuritis.
Conclusions: AQP4-specific T cells can enter the CNS to initiate clinical and histologic CNS disease, but are not sufficient to cause permanent damage. Retinal OCT can be used as a surrogate for CNS injury and neuronal loss in MOG and AQP4-targeted CNS autoimmunity in mice. Our models provide evidence that T cell mediated injury is not the basis for the tissue destructive pattern of damage seen in neuromyelitis optica.
Commercial Relationships: Andrés Cruz-Herranz, None; **Sharon A. Sagan**, None; **Ryan Winger**, None; **Garrett M. Timmons**, None; **Nicholas S. Baker**, None; **Michael P. Devereux**, None; **Marc H. Levin**, None; **Collin M. Spencer**, None; **Scott S. Zamvil**, None; **Ari J. Green**, None
Support: National Multiple Sclerosis Society Grant FG 20102-A-1

Program Number: 3328 **Poster Board Number:** B0604
Presentation Time: 11:00 AM–12:45 PM
Cultivation of mouse neural progenitor cells from the optic nerve
Rebecca J. Fawcett[1], Yan Guo[2], Candace Kerr[2], Steven L. Bernstein[1]. [1]Department of Ophthalmology and Visual Sciences, University of Maryland, Baltimore, MD; [2]Department of Biochemistry and Molecular Biology, Stem Cell Program, University of Maryland, Baltimore, MD.
Purpose: We previously reported expression of nestin and SOX-2 positive cells in the mouse optic nerve (ON)(Guo et al, ARVO 2015). These proteins are known to be localized in the CNS in neural progenitor cells found in the subventricular zone (SVZ) and in the hippocampus. We wanted to culture nestin/Sox 2(+) cells from the ON, and determine their growth potential and stem cell marker profile, in order to gain insight into the unique growth conditions that may aid in both self-renewal and ON repair
Methods: Optic nerve tissue was dissected, pooled and dissociated from 17-day old mice (n=8 mice/group), using collagenase. Cells were resuspended in supplemented serum-free neurobasal medium. Cell colonies were derived from the resuspended cells, and allowed to expand for various immunohistochemical, and molecular analyses. Cells were fixed *in situ* with paraformaldehyde and immunostained using nestin and SOX-2 antibodies, and visualized by confocal microscopic analysis. qPCR on first strand cDNA was performed to quantify levels of stem- and neural cell markers, and compared against freshly isolated ON and retina.
Results: Immunostaining of cultured cells showed positive co-expression for both nestin and SOX-2. In wells supplemented without serum in the presence of platelet-derived growth factor (PDGF), many, but not all ON-derived cells differentiated into olig1+, O4+ oligodendrocyte progenitors. RT-qPCR quantification of cDNA derived from mouse ON-derived cells revealed higher levels of nestin and Sox2, compared with ON and retinal tissue.
Conclusions: Cells derived from the mouse ON exhibit the capacity for self-renewal, similar to those seen for progenitors from other neural sources. These cells undergo successful continuous proliferation after 6 months. Our findings suggest a path for additional studies into ON-derived cells that may be useful in defining the unique conditions needed to obtain cells capable for studies into ON repair and regeneration.
Commercial Relationships: Rebecca J. Fawcett; **Yan Guo**, None; **Candace Kerr**, None; **Steven L. Bernstein**, None
Support: 2016-MSCRFF-2614, R01 EY015304 to SLB, Donner Foundation

Program Number: 3329 **Poster Board Number:** B0605
Presentation Time: 11:00 AM–12:45 PM
Sensory ocular dominance and area of the optic nerve head as measured by optical coherence tomography-a pilot study
Patricia Cisarik, Clint Prestwich. Southern College of Optometry, MEMPHIS, TN.
Purpose: Sensory ocular dominance can be very asymmetric, hardly discernable, or somewhere in between. Factors that determine sensory ocular dominance have yet to be completely determined. A relationship between anisometropia and sensory ocular dominance has been shown. Greater asymmetry in ocular dominance may develop in axial anisometropia due to a difference in optic nerve size, which may lead to a difference in signal strength to the brain from the two eyes. Whether a relationship exists between sensory ocular

dominance and anatomic parameters of the optic nerve head (ONH) as measured by optical coherence tomography (OCT) is unknown.
Methods: Sensory ocular dominance was determined for 85 young healthy adults, aged 20-35 years, without amblyopia, using the +2.00D monocular blur during binocular viewing test. Area of both optic nerve heads (ONH) of each subject was measured by spectral domain optical coherence tomography (SD-OCT). Subjects with ocular dominance were assigned to 1 of 2 groups: dominant eye larger (DEL), non-dominant eye larger (NDEL). The binomial probability that the sensory dominant eye would be the same as the eye with the larger area ONH by OCT was calculated.
Results: Sensory ocular dominance was identified in 70 subjects (82.4%); 15 subjects did not manifest a preferred eye. Forty-three of subjects manifesting a sensory dominant eye (61.4%) had sensory dominance identified for the eye with the larger ONH by OCT. The test of binomial probabilities showed that the likelihood of occurrence of this proportion (or greater) of subjects with sensory ocular dominance manifested by the eye with the larger ONH area by OCT is greater than chance ($p = 0.036$; $z = 1.79$).
Conclusions: Our pilot data on the relationship between sensory ocular dominance and ONH area measured by OCT suggests qualitatively that an interocular difference in optic nerve size may be a contributing factor to the establishment of which eye demonstrates sensory ocular dominance as assessed by the +2.00 monocular blur test. Whether similar findings with other tests of sensory dominance is unknown. A larger study of multifactorial contributions to sensory ocular dominance that includes evaluation of ONH anatomy and function is indicated.
Commercial Relationships: Patricia Cisarik, None;
Clint Prestwich, None